EARTH SURFACE PROCESSES AND LANDFORMS, VOL 23, 261–270 (1998)

BEDROCK SURFACE ROUGHNESS AND THE DISTRIBUTION OF SUBGLACIALLY PRECIPITATED CARBONATE DEPOSITS: IMPLICATIONS FOR FORMATION AT GLACIER DE TSANFLEURON, SWITZERLAND

BRYN HUBBARD[1]* AND ALUN HUBBARD[2]

[1]*Centre for Glaciology, Institute of Geography and Earth Sciences, University of Wales, Aberystwyth, Ceredigion, SY23, 3DB, UK*
[2]*Department of Geography, University of Edinburgh, Drummond Street, Edinburgh, EH8 9XP, UK*

Received 5 April 1997; Revised 1 July 1997; Accepted 16 July 1997

ABSTRACT

Two carbonate deposits are identified on the exposed bedrock surface in the forefield of Glacier de Tsanfleuron, Switzerland: macrocrystalline sparite and microcrystalline micrite. Comparison of the distributions of these forms with lee-side slope facets identified by high-pass filtering of a flow-parallel bedrock profile at a range of frequencies reveals two significant results. First, while the distribution of sparite is consistent with formation in the lee side of subglacial bedrock hummocks, that of micrite is not. This contrasts with previous investigations in which both sparite and micrite have been considered to form by mineral concentration and precipitation during the refreezing of regelation-related basal meltwaters in the lee side of bedrock hummocks. Alternative mechanisms of micrite formation involving carbonate deposition and/or precipitation within subglacial bedrock hollows are proposed. Second, the distribution of sparite is most strongly correlated with the distribution of lee-side slope facets identified by filtering at a frequency equivalent to a hummock wavelength of *c*. 0·1m. This correspondence indicates empirically that pressure-related melting and refreezing (regelation) operates most effectively around bedrock hummocks that are shorter than *c*. 0·1m. © 1997 John Wiley & Sons, Ltd.

Earth surf. process. landforms, **23,** 261–270 (1998)
KEY WORDS: bedrock roughness; subglacial carbonate precipitates; regelation

INTRODUCTION

Laminated carbonate crusts are frequently revealed on limestone bedrock surfaces exposed by recent glacier retreat (Figure 1). The morphology and composition of these crusts have been interpreted in terms of formation by solute concentration and mineral precipitation during the refreezing of meltwater films at the former glacier base (Hallet, 1976). Such films are considered to form by the melting of temperate basal ice (at its pressure melting temperature) as its pressure is raised on the upstream side of bedrock protuberances. The resulting meltwater is driven as a film to the lee side of the bedrock hummock, where the pressure is reduced, the melting point once again raised and the water refreezes. Refreezing releases latent heat of fusion, which is conducted back through the rock to the stoss face, where it fuels further melting. Since heat transfer is most effective over short distances, the rate of this melting–refreezing process (termed *regelation*) is considered to scale inversely with the size of the hummock involved (Weertman, 1957, 1964). Where such a process operates over limestones, the meltwater film comes into contact with freshly eroded carbonate dust and acquires a solute load that is dominated by Ca^{2+} and HCO^{-}_{3}. Carbonate then precipitates from solution during refreezing due to the progressive concentration of these species as solutes are rejected from the ice–water interface and degassing occurs (Hallet, 1976). This interpretation is generally consistent with the bulk ionic and isotopic compositions of subglacially precipitated carbonate crusts (e.g. Hanshaw and Hallet, 1978; Lemmens *et al*., 1982; Souchez and Lemmens, 1985), although non-equilibrium isotopic partitioning between aqueous, gaseous and solid phases may complicate these interpretations at high freezing rates (Clark and Lauriol, 1992; Fairchild *et al*., 1996).

Correspondence to: B. Hubbard
Contract grant sponsors: University of Wales Research Fund; Nuffield Foundation

CCC 0197-9337/98/030261–10 $17.50

Figure 1. Carbonate crusts deposited on Cretaceous limestone bedrock in the forefield of Glacier de Tsanfleuron. Sparite is located on the exposed surface to the left of the figure and micrite as a thicker deposit within the hollow to the right (in this case some post-glacial, subaerial weathering of the latter is evident). Former basal sliding direction was from left to right, as indicated by the orientation of the sparite spicules

Sharp *et al*. (1990) tested and refined this interpretation on the basis of the appearance, structure and elemental and isotopic composition of carbonate crusts exposed on a recently deglaciated proglacial bedrock surface at Glacier de Tsanfleuron, Switzerland. These authors classified the majority of deposits as two distinct forms: relatively thin, macrocrystalline *sparite* and relatively thick, microcrystalline *micrite*. The chemical composition of sparite and micrite was interpreted in terms of an evolutionary progression related to the stage of freezing at which precipitation occurred. Sparite, which is relatively ^{18}O-rich and low in Si, Fe and Mg, was considered to form under freely draining ('open-system') hydrological conditions or early on in the freezing of a closed reservoir. In contrast, relatively ^{16}O-rich and impure micrite was considered to form during the later stages of closed-system freezing. Thus, while sparite and micrite are morphologically distinctive, their chemistries have been interpreted in terms of an evolutionary series. In this paper we attempt to test this hypothesized mode of formation by comparing the distribution of precipitates over a proglacial bedrock profile at Glacier de Tsanfleuron with the locations at which regelation-related refreezing would be expected to occur in the absence of basal cavitation. If the interpretation of Sharp *et al*. (1990) is correct then the actual distribution of both micrite and sparite will correspond closely with predicted locations of regelation-related refreezing (the lee sides of small-scale bedrock hummocks). However, if such a correspondence is not found for sparite and/or micrite then some refinement of this interpretation may be justified.

FIELDSITE AND METHODS

Glacier de Tsanfleuron is a 4 km^2 plateau glacier located between *c*. 2420 and *c*. 2850 m a.s.l. to the northwest of Sion, Switzerland (Figure 2). The glacier has been extensively studied, mainly in terms of the relationship between its basal ice layers (Lemmens *et al*., 1982; Souchez and Lemmens, 1985; Tison and Lorrain, 1987; Hubbard and Sharp, 1995) and the carbonate crusts deposited on the Urgonian (Cretaceous) limestone bedrock revealed by its post-Little Ice Age retreat. The present study site is located on this plateau, some 20 to 30 m from

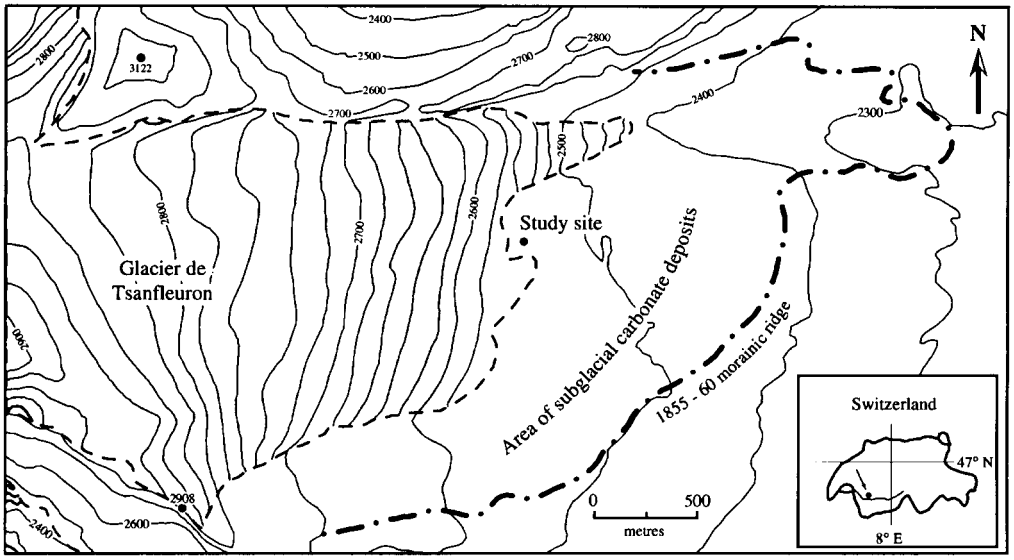

Figure 2. The proglacial study site at Glacier de Tsanfleuron, Switzerland. The study site is located at approximately (5850, 1300) on the Swiss Grid

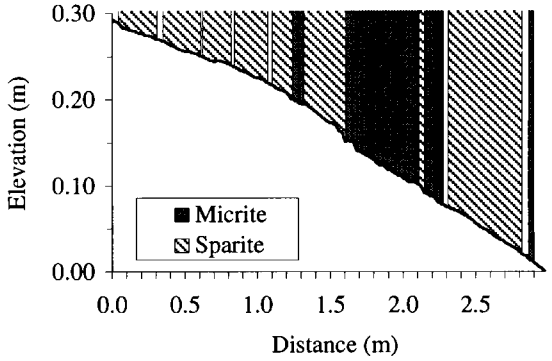

Figure 3. Observed distributions of sparite and micrite over the raw bedrock elevation profile

the glacier margin (Figure 2), having been exposed to subaerial weathering for *c*. 10 years (M-T. Diet, unpublished). The study involved the following stages.

(i) The character, distribution and topographic setting of carbonate deposits was observed over the entire proglacial bedrock area.

(ii) The distribution of the carbonate deposits identified in (i) was mapped at a point spacing of 0·01 m over a 3 m long, linear bedrock profile aligned parallel to the former glacier sliding direction (as indicated by the orientation of sparite crystals and bedrock striations in the area) (Figure 3).

(iii) The bedrock surface was surveyed (Figure 4a) using a Geodimeter System 400 total station. Surveying accuracy was maximized by focusing on thin cross-hairs within a reflector prism securely mounted at the base of the survey staff. We believe this procedure rendered our operator-based (horizontal and vertical) errors within the manufacturer's instrument accuracy of 2 mm ± 3 ppm (Geodimeter, 1995). The survey station was located within 10 m of the profile, rendering the latter term about 30 μm. Where precipitates were formed, the profile recorded the upper surface of the precipitate and not the bedrock. This is not considered to influence the significance of the results since, in the absence of evidence for precipitate surface erosion along the profile, the existing precipitate surface was effectively acting as the substrate on which continued precipitation was occurring.

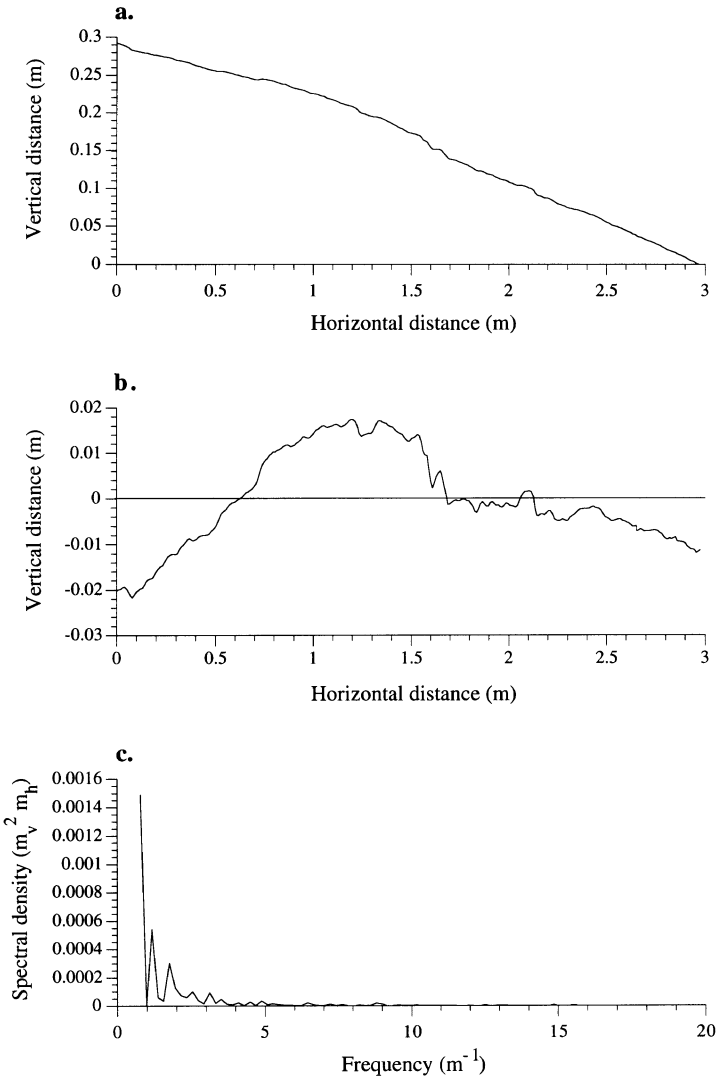

Figure 4. The bedrock profile studied: (a) raw bedrock elevations; (b) least-squares linear detrended elevations; and (c) the resulting power spectrum following fast Fourier transformation. Frequencies equivalent to wavelengths greater than 50 per cent of the profile length are omitted from (c)

(iv) The profile was linearly detrended (Figure 4b) (Hegge and Masselink, 1996) prior to transformation into the frequency domain using the fast Fourier transform (FFT) technique (Cooley and Tukey, 1965; MATLAB, 1992) (Figure 4c).

(v) Low frequency roughness elements were systematically removed from the resulting auto-spectrum using high-pass filters at cutoff wavelengths of 0·02, 0·04, 0·06, 0·08, 0·10, 0·12, 0·15, 0·20, 0·30, . . . 1·00 m. Hereafter, we refer to these frequency-based filter cutoffs in terms of their wavelength equivalents. A maximum wavelength cutoff of 1 m was chosen since this represents the theoretical upper boundary of hummock lengths around which regelation is expected to occur (e.g. Kamb, 1970), whilst still providing meaningful results, since it is less than one-half of the total profile length.

(vi) The resulting spectra were inverted to 3 m long, filtered profiles (Figure 5), from which the distribution of lee-side locations (defined as downglacier-facing facets) for each filter cutoff was identified and plotted (Figure 6).

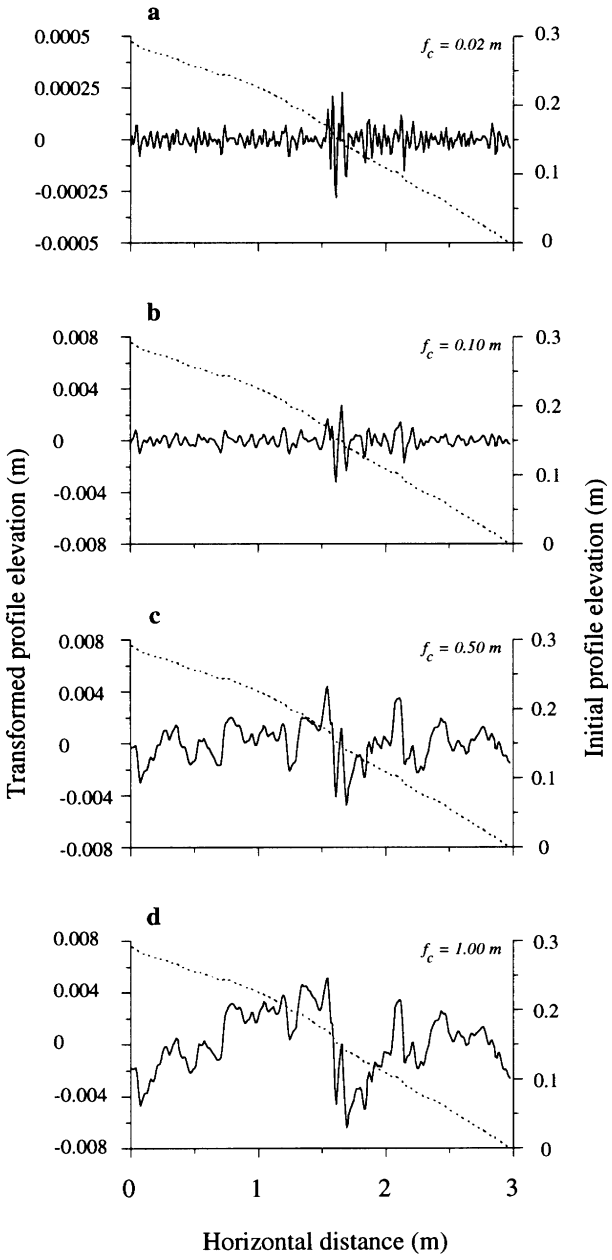

Figure 5. Fast Fourier transformed surfaces following high-pass filtering at wavelength cutoffs (f_c) of (a) 0·02 m, (b) 0·10 m, (c) 0·05 m and (d) 1·00 m. The initial profile (dashed) is presented for comparison

(vii) The distributions generated by (vi) were compared with the distribution of precipitates recorded over the bedrock profile in (ii). Comparison was made for each of the 300 cells via a simple binary fit relating lee-side slope facets on each of the filtered profiles to the presence of sparite or micrite deposits on the actual profile. Matching cells (lee-presence or stoss-absence) were assigned a value of 1 and non-matching cells (lee-absence or stoss-presence) a value of 0. The sum of the matching cells for each filtered bedrock profile was then expressed as a percentage of the total number of cells (300) (Figure 7).

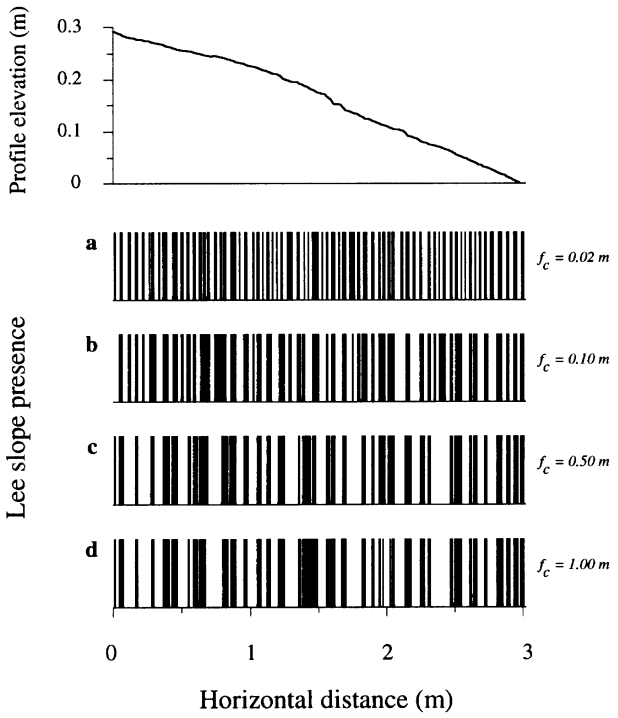

Figure 6. Lee-side (refreezing) locations reconstructed for a selection of transformed profiles: wavelength cutoffs (f_c) are (a) 0·02 m, (b) 0·10 m, (c) 0·50 m and (d) 1·00 m. Lee sides are depicted as solid bars. The initial profile is presented for comparison

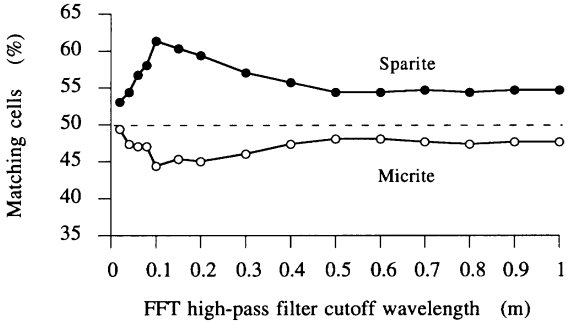

Figure 7. Fit between the actual distributions of sparite and micrite over the bedrock profile and predicted lee-side locations for a variety of high-pass filter cutoffs. Fitting procedure is described in the text

RESULTS

Both sparite and micrite could be clearly distinguished by eye in the forefield of Glacier de Tsanfleuron (Figure 1). Sparite was deposited in three principal totographic settings: as continuous coatings over large patches of relatively flat, abraded bedrock; on the lee faces of small bedrock irregularities located on the stoss faces of larger hummocks; and as thin ribbons on the rims of large bedrock hollows. In contrast, micrite was generally absent from flat, exposed bedrock areas. Instead, the deposit was distributed as smooth veneers covering relatively shallow bedrock hollows and as thicker masses extending into deep bedrock hollows

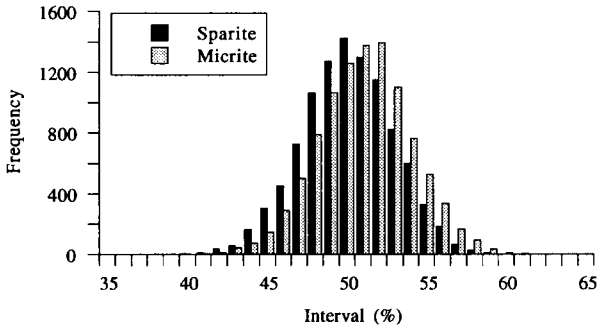

Figure 8. Frequency plots of the match between recorded sparite and micrite distributions and randomly redistributed lee-side locations predicted by the FFT high-pass filter with a wavelength cutoff of 0·10 m. Redistribution was repeated 10 000 times

(Figure 1). No observations were made of one deposit either overlying or interstratified with the other along the present profile. Although observed at Glacier de Tsanfleuron, such superimposed stratigraphies appear to be rare.

Field mapping of the bedrock profile revealed extensive sparite and micrite deposits, with only isolated, small patches of bare bedrock (Figure 3). No evidence of subaerial erosion of these calcite deposits, such as accordant rill development or exposed internal layering, was observed. The distribution of sparite and micrite over the profile is consistent with the qualitative observations made in the area: micrite is largely restricted to two extended hollows, from *c*. 1·25 to *c*. 1·35 m and *c*. 1·60 to *c*. 2·20 m, while sparite deposits coat much of the remaining bedrock surface (Figure 3). The bedrock profile studied has an elevation drop of *c*. 0·3 m and is characterized by surface undulations that are dominated by low-frequency elements (Figure 4). Such flow-parallel smoothing is consistent with previous investigations of glaciated bedrock (Sharp *et al*., 1989) and results from abrasive erosion of high-frequency irregularities by the former glacier (e.g. Boulton, 1979). Application of FFT high-pass filters to this profile reveals only those roughness elements that are of shorter wavelength than the filter cutoffs applied. Thus, the greater the filter cutoff wavelength, the larger the roughness elements revealed (Figure 5). Plots of the resulting lee-side locations for a selection of the filtered profiles (Figure 6) illustrate this effect, where the application of progressively lower-wavelength filter cutoffs results in an increase in the number and a reduction in the length of individual lee- and stoss-side facets.

Comparison of the refreezing locations predicted on the basis of the filtered profiles with the observed distributions of sparite and micrite over the initial bedrock profile (Figure 7) reveals two notable features. First, predicted refreezing locations are more strongly associated with the actual distribution of sparite than with the actual distribution of micrite. The percentage fit for the former varies between *c*. 53 and 62 per cent and that of the latter between *c*. 44 and 49 per cent. Relative to random distributions (*c*. 50 per cent fit), these data therefore indicate a positive association between sparite distribution and predicted refreezing locations and a negative association between micrite distribution and predicted refreezing locations. Second, the degree of fit between the actual and predicted regelation-related precipitation locations varies systematically with the wavelength of the filter applied. The best fit for sparite (*c*. 62 per cent) and the worst fit for micrite (*c*. 44 per cent) both occur at a cutoff wavelength of 0·10 m (Figure 7).

The significance of these patterns may be assessed statistically through a Monte Carlo-type simulation. Of the 300 total (1 cm long) cells, 146 were identified as lee sides following the application of the 0·1 m FFT filter. We randomly redistributed these 146 cells over the 300 cell profile 10 000 times and recorded the percentage fit with the actual distributions of sparite and micrite (as described above) for each run. Results provide statistical distributions of the goodness of fit of both sparite and micrite with the randomly redistributed lee-side locations (Figure 8). As expected, both distributions approximate normality: the mean value of the fit for sparite is 49·6 per cent ($\sigma = 2{\cdot}9$ per cent) and for micrite 50·6 per cent ($\sigma = 2{\cdot}9$ per cent). Z-score analysis indicates that the probability of a sparite fit of 62 per cent and a micrite fit of 44 per cent being achieved by a chance redistribution of the lee-side refreezing locations is <0·01 in both cases. It is therefore highly unlikely that the recorded match between the distribution of either of the carbonate deposits and lee-side locations (following filtering at a wavelength of 0·1 m) is due to chance.

DISCUSSION

General observations of the distribution of sparite and micrite suggest that the association of the latter with regelation-related refreezing may be problematic, since such refreezing would be expected only at the rims of shallow bedrock hollows rather than across their entire surfaces, as the observed distribution of micrite suggests. This qualitative inference is strengthened by the statistically poor association of micrite with lee-side roughness elements on the filtered profiles. In contrast, sparite, which is observed more generally over exposed bedrock surfaces, is strongly associated with lee-side locations on the filtered profiles. Sparite distribution is therefore consistent with an origin associated with regelation-related refreezing. If this association is accepted, then the comparison of sparite deposits with filtered roughness facets indicates that this refreezing operates most effectively around bedrock roughness elements with a wavelength of *c*. 0·1m at Glacier de Tsanfleuron. This correspondence is consistent with theoretical predictions of more active regelation at progressively small bedrock roughness scales (e.g. Weertman, 1957; Nye, 1969; Lliboutry, 1975; Kamb, 1970; Fowler, 1981) since the presence of carbonate deposits indicates locations of net refreezing rather than locations of maximum precipitation. While the latter could potentially be investigated via an analysis of the thickness of precipitate crusts at various locations, the present study was concerned only with the presence or absence of such deposits. Our data therefore indicate that, in reality, bedrock hummock stoss faces with a wavelength smaller than *c*. 0·1m may at least intermittently act as sites of regelation refreezing (being located in the lee of larger bumps around which ice is regelating). A 0·1m bump wavelength is associated with a vertical relief of *c*. 0·008 m at Glacier de Tsanfleuron (Figure 5b). This thickness is consistent with both theoretical (e.g. Nye, 1970) and empirical (e.g. Kamb and LcChapelle, 1964; Hubbard and Sharp, 1993) reconstructions of the thickness of undeformed regelation-related ice layers.

In the most detailed analysis of subglacial carbonate deposits to date, Sharp *et al*. (1990) provide strong evidence that, relative to sparite, micrites (i) are dominated by carbonate that is low in $\delta^{18}O$ and δD, (ii) contain high proportions of impurities and detrital clasts, and (iii) are characterized by repeated internal laminations. Sharp *et al*. (1990) interpret these characteristics in terms of the formation of sparite from open-system, through-flowing waters and micrite from closing- or closed-system, regelation waters. In contrast, our data indicate that sparite is formed by closed-system regelation-related refreezing, and that micrite is principally formed in bedrock hollows that are not normally associated with cavity-free, regelation-related refreezing. Some revision of the interpretation of Sharp *et al*. (1990) may therefore be required. While ascribing a precise origin to micrite deposits is beyond the scope of the present paper, some potential modes of formation may be proposed that are consistent with both our data and those of Sharp *et al*. (1990). First, externally formed carbonate particles may be flushed into and deposited on the floor of subglacial bedrock hollows. In addition to detrital material, these particles may be largely derived from the overlying, debris-bearing basal ice. Fairchild *et al*. (1993) identified fine-fraction carbonate precipitates in basal ice debris at Glacier de Tsanfleuron. Such intra-ice precipitation may be induced by pressure and water-ice phase changes induced by the passage of temperate ice over a rigid and rough bedrock substrate (e.g. Lliboutry, 1993; Hubbard and Sharp, 1995; Jansson *et al*., 1996). Deposited carbonates may thereby progressively build up in bedrock hollows until they solidify upon exposure to air as the glacier retreats and thins above them. Such a mechanism of formation is consistent with the presence of a detrital component in micrite deposits, their laminated internal structure, their formation in subglacial bedrock hollows and their isotopically 'evolved' composition (consistent with precipitation from waters that have already experienced partial refreezing, as expected in the basal ice layers).

Second, carbonate precipitation may occur in subglacial hollows, formed where the glacier separates from its substrate, as a result of the degassing of influent $CaCO_3$-saturated basal meltwaters. Here, degassing may be associated with meltwater freezing (Fairchild *et al*., 1996) and/or a fall in pressure relative to the drainage pathways via which the meltwaters were delivered to the cavity. Again, detrital clasts may be introduced by isotopically light influent meltwaters supplied by multiple, upglacier regelation cycles (Hubbard and Sharp, 1993). However, interpreation of the (*C* and *O*) isotopic composition of such carbonate deposits may be complicated by the possibility of non-equilibrium precipitation during rapid, freezing-related degassing. In such situations, the preferential incorporation of light isotopes into the gas phase may cause preciptiated $CaCO_3$ to be isotopically heavy relative to its theoretical equilibrium composition (Clark and Lauriol, 1992;

Fairchild *et al*., 1996). However, the precise influence of such processes remains to be tested in subglacial environments. Heat-sinks for the freezing of meltwaters trapped in bedrock hollows at otherwise predominantly temperate-based glaciers may be provided by the penetration of the winter cold wave through the overlying ice (e.g. Weertman, 1961) or the influx of cold external air (e.g. Anderson *et al*., 1982). Both of these processes are restricted to a zone close to the glacier margins, where such cavities are likely to be only partially water-filled. Such deposition from waters flowing at atmospheric pressure may explain the (constructional) furrows that characterize the upper surface of many micrite deposits (e.g. Hallet, 1976). More rare, smooth-surfaced micrite deposits may reflect intermittent degassing and/or freezing-related precipitation and deposition through the water column in water-filled cavities.

CONCLUSIONS

A number of conclusions may tentatively be advanced on the basis of the present study.

(i) Observational evidence indicates that the distinction between sparite and micrite is real and that both exist in the forefield of Glacier de Tsanfleuron, Switzerland. Sparite is predominantly deposited on smoothed and exposed bedrock surfaces and micrite in bedrock hollows.

(ii) Detailed analysis of the distribution of these carbonate forms in relation to bedrock roughness elements indicates that sparite may be formed in response to regelation-related refreezing around bumps where ice is in intimate contact with its bed. In contrast, the distribution of micrite is not consistent with such a mode of formation. Instead, micrite deposits appear to be predominantly formed within subglacial cavities, either by the influx and deposition of carbonate material or by local carbonate precipitation in response to net freezing and/or CO_2 degassing.

(iii) The closed-system regelation process that we consider to be responsible for the formation of sparite operates most effectively around bedrock roughness elements with wavelengths up to *c*. 0·1 m (amplitude *c*. 0·008 m). This is consistent with earlier theoretical predictions and empirical observations.

ACKNOWLEDGEMENTS

Our thanks are extended to Peter Nienow and the staff of Cabane Prarochet, Tsanfleuron, for logistical assistance and to Martin Sharp, Ian Fairchild, Urs Fischer and Martin Siegert for helpful suggestions. Research was supported by the University of Wales Research Fund and the Nuffield Foundation.

REFERENCES

Anderson, R. S., Hallet, B., Walder, J. and Aubry, B. F. 1982. 'Observations in a cavity beneath Grinnell Galcier', *Earth Surface Processes and Landforms*, **7**, 63–70.

Boulton, G. S. 1979. 'Processes of glacier erosion on different substrata', *Journal of Glaciology*, **23**, 15–38.

Clark, I. D. and Lauriol, B. 1992. 'Kinetic enrichment of stable isotopes in cryogenic calcites', *Chemical Geology*, **102**, 217–228.

Cooley, J. W. and Tukey, J. W. 1965. 'An algorithm for the machine calculation of complex Fourier series'. *Mathematics of Computation*, **19**, 297–301.

Fairchild, I. J., Bradby, L. and Spiro, B. 1993. 'Carbonate diagenesis in ice', *Geology*, **21**, 901–904.

Fairchild, I. J., Killawee, J. A. and Spiro, B. 1996. 'Calcite precipitates formed by freezing processes: kinetic controls on morphology and geochemistry', *Proceedings of the Fourth International Symposium on the Geochemistry of the Earth's Surface*, 178–183.

Fowler, A. C. 1981. 'A theoretical treatment of the sliding of glaciers in the absence of cavitation', *Philosophical Transactions of the Royal Society of London, Ser. A.* **298**, 637–685.

Geodimeter. 1995. *Geodimeter News*, Geotronics Limited, UK, **3**, 8 pp.

Hallet, B. 1976. 'Deposits formed by subglacial precipitation of $CaCO_3$', *Geological Society of America Bulletin*, **87**, 1003–1015.

Hanshaw, B. B. and Hallet, B. 1978. 'Oxygen isotope composition of subglacially precipitated calcite: possible palaeoclimatic implications', *Science*, **200**, 1267–1270.

' Hegge, B. J. and Masselink, G. 1996. 'Spectral analysis of geomorphic time series: auto-spectrum'. *Earth Surface Processes and Landforms*, **21**, 1021–1040.

Hubbard, B. and Sharp. M. 1993. 'Weertman regelation, multiple refreezing events and the isotopic evolution of the basal ice layer', *Journal of Glaciology*, **39**, 275–291.

Hubbard, B. and Sharp, M. 1995. 'Basal ice facies and their formation in the western Alps', *Arctic and Alpine Research*, **27**, 301–310.

Jansson, P., Kohler, J. and Pohjola, V. A. 1996. 'Characteristics of basal ice at Engabreen, northern Norway', *Annals of Glaciology*, **22**, 114–120.

Kamb, B. 1970. 'Sliding motion of glaciers: theory and observation', *Reviews in Geophysics and Space Physics*, **8**, 673–728.
Kamb, B. and LaChapelle, E. 1964. 'Direct observation of the mechanism of glacier sliding over bedrock', *Journal of Glaciology*, **5**, 159–172.
Lemmens, M., Lorrain, R. and Haren, J. 1982. 'Isotopic composition of ice and subglacially precipitated calcite in an alpine area', *Zeitschrift für Gletscherkunde und Glazialgeologie*, **18**, 151–159.
Lliboutry, L. 1975. 'Loi de glissement d'un glacier sans cavitation', *Annales de Géophysique*, **31**, 207–226.
Lliboutry, L. 1993. 'Internal melting and ice accretion at the bottom of temperate glaciers', *Journal of Glaciology*, **39**, 50–64.
MATLAB. 1992. *MATLAB for UNIX workstations: User's Guide*, MathWorks Inc., Mass. USA.
Morland, L. W. 1976. 'Glacier sliding down an inclined wavy bed', *Journal of Glaciology*, **17**, 447–462.
Nye, J. F. 1969. 'A calculation on the sliding ice over a wavy surface using a Newtonian viscous approximation', *Proceedings of the Royal Society of London. Series A.* **311**, 445–467.
Nye, J. F. 1970. 'Glacier sliding without cavitation in a linear viscous approximation', *Proceedings of the Royal Society of London, Series A*, **315**, 381–403.
Paterson, W. S. B. 1994. *The Physics of Glaciers*, Pergamon, Oxford, 480 pp.
Sharp, M. J., Dowdeswell, J. A. and Gemmell, J. C. 1989. 'Reconstructing past glacier dynamics and erosion from glacial geomorphic evidence: Snowdon, North Wales', *Journal of Quaternary Science*, **4**, 115–130.
Sharp, M. J., Tison, J. -L. and Fierens, G. 1990. 'Geochemistry of subglacial calcites: implications for the subglacial hydrology of the basal water film', *Arctic and Alpine Research*, **22**, 141–152.
Souchez, R. A. and Lemmens, M. M. 1985. 'Subglacial carbonate deposition: an isotopic study of a present-day case', *Palaeogeography, Palaeoclimatology and Palaeoecology*, **51**, 357–364.
Tison, J. -L. and Lorrain, R. D. 1987. 'A mechanism of basal ice formation involving major ice-fabric changes', *Journal of Glaciology*, **33**, 47–50.
Weertman, J. 1957. 'On the sliding of glaciers', *Journal of Glaciology*, **3**, 33–38.
Weertman, J. 1961. 'Mechanism for the formation of inner moraines found near the edge of cold ice caps and ice sheets', *Journal of Glaciology*, **3**, 965–978.
Weertman, J. 1964. 'The theory of glacier sliding', *Journal of Glaciology*, **5**, 287–303.

